EXPERIMENTAL AND MODEL BASED PERFORMANCE INVESTIGATION OF A SOLID DESICCANT WHEEL DEHUMIDIFIER IN SUBTROPICAL CLIMATE

by

Ghulam Qadar CHAUDHARY[a], Muzaffar ALI[a], Muhammad ASHIQ[a], Hafiz Muhammad ALI[a*], and Khuram Pervez AMBER[b]

[a] Department of Mechanical Engineering, University of Engineering and Technology, Taxila, Punjab, Pakistan
[b] Department of Mechanical Engineering, Mirpur University of Science and Technology, Mirpur, AJK, Pakistan

Original scientific paper
https://doi.org/10.2298/TSCI170127165C

This paper presents real time performance analysis of a silica gel based desiccant wheel dehumidifier. Thermodynamic model is also validated through comparison under a wide range of operating conditions for subtropical climate conditions. Initially, a mathematical model is developed by using various set of equations for desiccant wheel dehumidifier in engineering equation solver. Afterwards, a parametric analysis of the system is performed including various design and climate parameters such as: inlet air humidity ratio, inlet air temperature, regeneration inlet humidity ratio, regeneration temperature, and rotation speed of the wheel. Then, an experimental set-up of the system is established in Taxila Pakistan for the real-time performance assessment. The results revealed that the optimal rotation speed of desiccant wheel ranged from 15-17 rph. The maximum model based and experimental effectiveness is 0.45 and 0.43, respectively at regeneration temperature of 80 °C. The maximum and minimum root mean square error values for effectiveness are 3.2% and 2.1%, respectively. Thus, the comparison between experimental and model results showed a good agreement.

Key words: *solid desiccant wheel, comparative performance analysis, engineering equation solver, parametric analysis, dehumidification, subtropical climate*

Introduction

The effective control of indoor humidity is a significant aspect for thermal comfort of domestic, commercial, and industrial buildings. Thermal comfort includes temperature and relative humidity as key parameters of the conditioned space. However, acute levels of relative humidity in various applications can disturb individuals comfort [1]. Furthermore, uncontrolled moisture in air additionally influence the human health issues [2]. While negative effect of higher humid levels on building materials also causes electrochemical corrosion, volume changes, and chemical disintegration [3]. Therefore, in order to overcome negative effects of elevated humidity levels, indoor humidity should have to be controlled either by conventional or non-conventional methods.

* Corresponding author, e-mail: h.m.ali@uettaxila.edu.pk

In humid climates, controlling high humidity levels is a major contributor to energy consumption in HVAC appliances due to high latent load [4]. Most conventional cooling systems intended for effective control of air temperature rather than humidity. The air dehumidification using conventional techniques such as vapor compression systems is achieved by cooling the outside air below its dew point temperature. However, the dehumidified air is needed to be reheated again to comfort temperature that causes additional energy input [5, 6].

Therefore, the researchers focus is shifted towards more energy efficient methods, such as desiccant dehumidification for controlling indoor humidity without additional energy consumption [7, 8]. Both liquid and solid desiccant based systems are utilized for dehumidification application [7, 9]. Desiccant based dehumidification offers utilization of waste heat as well as appropriate for solar thermal assisted application [9]. However, the solid desiccant wheel is generally used to control the humidity of air in the cooling systems [10].

Dehumidification process is strongly affected by temperature, moisture and air speed along with rotation speed of the wheel. However, the regeneration air temperature must be changed in accordance with the regeneration properties of material used for dehumidification [11].

Several studies focused on simplified techniques for performance evaluation of desiccant wheels [12, 13]. In these research studies experimental co-relations were proposed based on supplied manufacturer data. However, air face velocity and wheel revolution speed were ignored in modeling. In another research study the performance of desiccant wheel is evaluated at constant air velocity and wheel speed and found that effectiveness remains unchanged over wide operating conditions [14]. Similarly, evaluation of desiccant dehumidification capacity through humidity ratio as well as temperature effectiveness indices is proposed in the studies [15-17].

Although desiccant wheel is a key component of desiccant evaporative cooling (DEC) system, but analysis of complete cooling system is often focused instead of comprehensive analysis of individual desiccant component [18-23]. Furthermore, precise prediction of desiccant wheel performance in transient energy system simulations for DEC systems is also of prime importance. However, majority of parametric analysis are based on theoretical studies using governing equations with certain assumptions which do not represent the actual performance under real conditions.

Similarly, the manufacturer data in terms of performance curves is based on design conditions and sometime does not capture the complete local conditions when subjected to transient analysis. Additionally, keeping in view that climate imposes its own conditions. The current study analyzed the complete climate range in subtropical climate conditions which could be equally applicable to many countries in the Asian region.

Therefore, the current model development and its validation through comprehensive experimentation are carried out for all influencing operating conditions in subtropical climate of Taxila city, Pakistan. Additionally, it is also observed that built in thermodynamic models of desiccant wheel like in TRNSYS library are capable of producing regeneration temperature as an output, while outlet temperature and humidity is often desired against a regeneration temperature. Finally, the proposed model can precisely measure the outlet conditions on process as well as regeneration sides and offers an effective future application for energy system simulation programs that are compatible for coupling with engineering equation solver like TRNSYS.

Mathematical model of desiccant wheel

The mathematical model of desiccant wheel is based on various set of algebraic equations for determining absolute humidity and temperature on process as well as regeneration side. Furthermore, additional correlations are also used to find moist air specific properties under wide range of operating conditions such as specific enthalpy to temperature, and relative humidity to humidity ratio. Total amount of moisture adsorbed in the desiccant wheel is determined through adsorption isotherms [24]. Adsorption material strongly influences these isotherms along with inlet humidity [25, 26]. Adsorption isotherms characterize the amount of water absorbed by desiccant wheel and depend upon adsorbent material. Therefore, to determine the equilibrium amount of moisture adsorbed, q_{eq}, as a function of relative humidity, Freundlich eq. (1) is used:

$$q_{eq} = C(RH)_{in}^{1/n} \tag{1}$$

The isosteric heat of adsorption is found by using Clausius-Clapeyron relationship, whose range is in between 2100 kJ/kg and 2300 kJ/kg. The surface diffusivity is linked with temperature via Arrhenius eq. (2) which is used to calculate the activation energy for diffusion. This activation energy is about 80% of isosteric heat of adsorption and offers a good realistic estimate [27]:

$$D_{sf} = 2.27 \cdot 10^{-7} \exp\left[\frac{E_{at}}{R\left(\frac{T_{sin} + T_{reg}}{2}\right)}\right] \tag{2}$$

Additionally, sensible heat exchange between the process and regeneration side through wheel rotation per unit time is determined by eq. (3) [26]:

$$H_1 = \frac{\rho_{dw} C_{pc} (T_{reg} - T_{sin}) NL}{\beta_s \rho_a U_s} \tag{3}$$

Majority of mathematical models for desiccant wheel can be categorized into two types.

– The model that considers the heat and mass transfer resistance offered by the bulk gas, while ignoring the resistance offered by the solid material of the wheel.
– The model that considers both resistances such as solid side and bulk gas molecules

The current model is modified and calculates the mass transfer by considering the surface diffusion as dominant factor. Therefore, the amount of water vapor adsorbed by the adsorbent material is given by eq (4):

$$q = 1.129 \sqrt{D_{sf} t_1} \rho_{ad} A_{ws} q_{eq} \tag{4}$$

where t_1 is the adsorption time which is computed by $t_1 = 3600\ B_s/N_w$. Subsequently, hourly measurements of water exchange from process air to the regeneration air through the desiccant wheel are determined by eq. (5):

$$Q_m = qSL\rho_{dw} N \tag{5}$$

The conditions at outlet of process and regeneration stream depend upon heat and mass transfer as given in the eqs. (3) and (5). Absolute humidity ratio on process outlet side is calculated by eq. (6):

$$W_{\text{sout}} = W_{\text{sin}} - \frac{Q_{\text{m}}}{\dot{m}_{\text{s}}} \tag{6}$$

where $\dot{m}_{\text{s}}$ is the mass-flow rate of process air and is determined by eq. (7):

$$\dot{m}_{\text{s}} = \rho_{\text{a}} U_{\text{s}} S \tag{7}$$

Enthalpy and temperature of the process air at outlet are determined using eqs. (8) and (9):

$$h_{\text{sout}} = h_{\text{sin}} + H_1 \tag{8}$$

$$T_{\text{sout}} = \frac{h_{\text{sout}} - 2501 W_{\text{sout}}}{1.86 W_{\text{sout}} + 1.006} + 273.15 \tag{9}$$

The dehumidification effectiveness of the desiccant wheel is defined as the ratio of dehumidification achieved from desiccant wheel to the inlet humidity when ideal humidity at outlet is considered to be zero. The parameter is given as eq. (10) [17]:

$$\varepsilon_{\text{d}} = \frac{W_{\text{sin}} - W_{\text{sout}}}{W_{\text{sout}} - W_{\text{ideal}}} \tag{10}$$

where W_{ideal} is the specific humidity of the air at desiccant wheel outlet. If its value is considered to be zero it will represent an ideal wheel that will completely dehumidify the air. The present model is modular that is flexible to adopt different values of design parameters. However, geometric and thermodynamic properties of desiccant wheel subjected to theoretical and experimental parametric analysis are mentioned in tab. 1 [25, 28].

Table 1. Thermodynamic and other properties of desiccant wheel

Parameters	Design values	Parameters	Design values
Desiccant wheel material	Silica gel	Surface area of desiccant wheel, A_{ws} [m^2/kg-wheel]	11
Wheel diameter, D [mm]	350	Adsorption isotherm constants:	
Wheel thickness, L [mm]	200	n [–]	1.5
Fractional area of process zone	0.465	C [–]	0.24
Overall cross-sectional area, A [m^2]	0.008	Density of adsorbent, ρ_{ad} [kgm^{-3}]	1200
Channel pitch, $a \times b$ [mm]	2.2 × 2	Activation energy, E_{at} [kJkg^{-1}]	1720
Bulk density, ρ_{ad} [kgm^{-3}]	270	Diffusion coefficient, D_0 [m^2s^{-1}]	$2.27 \cdot 10^7$
Specific surface area, A_{sp} [m^2m^{-3}]	3000	Specific heat capacity, C_{pc} [$\text{Jkg}^{-1}\text{K}^{-1}$]	921

Experimental analysis and model validation

The numbers of experiments are carried out to study the effect of various parameters in climate condition of Taxila city, Pakistan. Model results for each parameter are compared with published data, as well as experimental results. However, effectiveness is considered as critical parameter and validated with experimental results. The range of parameters for theoretical and experimental analysis is given in tab. 2.

The values during the parametric analysis of the model are same as ASHRAE study, except thermodynamic and geometric properties of the wheel. Furthermore, during comparative analysis and model validation baseline values of variables are considered.

Table 2. Range of parameters

	Theoretical analysis		Experimental analysis	
Parameters	Baseline values	Parametric variations	Baseline values	Parametric variations
Temperature of ambient air, T_{amb} [°C]	30	–	26	–
Humidity ratio of ambient air, W_{amb} [gkg^{-1}]	10	–	11	–
Inlet temperature of process air, T_{sin} [°C]	31	20-40	25	25-45
Inlet humidity ratio of process air, W_{sin}, [gkg^{-1}]	8.0	4-12	12	12-18
Superficial velocity of process air, $\dot{m}_s$ [ms^{-1}]	2	1-3.5	2	–
Regeneration air temperature, T_{reg} [°C]	81	45-120	80	50-80
Inlet humidity ratio of regeneration air, W_{reg} [gkg^{-1}]	12.5	–	12	–
Rotation speed, N [r per hour]	15	15-36	17	10-40

Experimental set-up

Experimental set-up consists of a desiccant wheel, hot water tank, heating coils, and humidifiers along with sensing and measuring instruments. The hot water tank is equipped with electric heaters, temperature, and flow controller. The casing of the wheel is divided in two sections, one is the regeneration zone regenerated by warm air stream and the other is a process or adsorption zone where the inlet air stream is dehumidified. As the current study is designed to perform real time parametric analysis so heating coils and humidifiers are present on both process as well as regeneration streams. Process air enters at Stage 1, passes through the heating coil and humidifier to achieve the desired moist air properties at Stage 2. Afterwards, air passes through the desiccant wheel that absorbs the moisture present in the air. Finally, dehumidified warm air is obtained at Stage 3.

Similarly, regeneration air appears at Stage 4, passes through heating coil and humidifier to achieve the desired regeneration air properties. Afterwards, air passes through the main heating coil at Stage 5 to raise the regeneration temperature to the desired regeneration value. Experimental data is considered for analysis after system reaches its steady state condition. A complete overview of the experimental set-up along with instrumentation is shown in fig. 1.

The process and regeneration air are supplied by individual axial fans. Desiccant wheel is equipped with variable speed motor. The relative humidity and temperature at every section are measured by hygrometer and temperature probes, respectively. The temperature of both air streams in the range of 20-80 °C are measured by using K-type thermocouples with sensitivity of

0.01 °C and accuracy of ±0.01. Relative humidity is measured with type EFK-E1S sensor calibrated with standard hygrometer. Air velocity and wheel revolutions are measured by anemometer and tachometer respectively. The physical system is as shown in fig. 2.

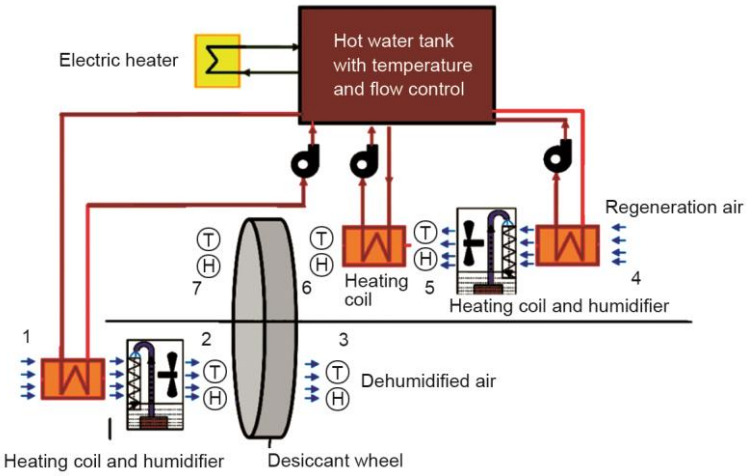

Figure 1. Schematic of experimental set-up along with measuring and sensing instrument

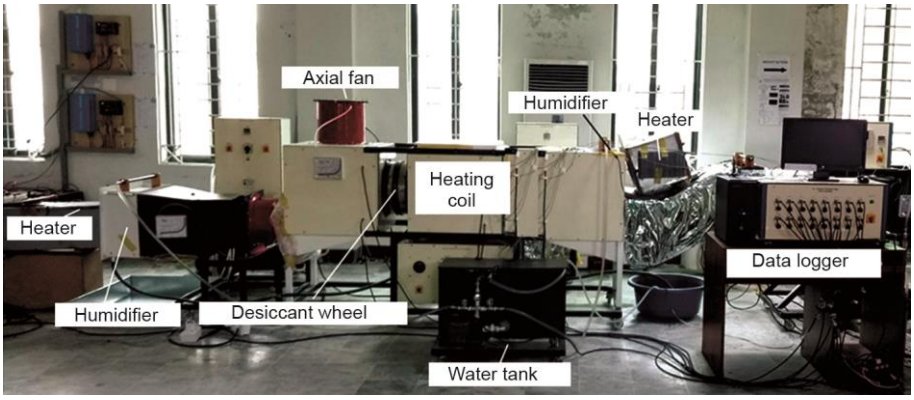

Figure 2. Physical set-up of desiccant dehumidification system

Results and discussion

In current study, a real time parametric analysis of silica gel desiccant wheel dehumidifier is carried out along with model validation under a wide range of design and operating conditions. Desiccant wheel performance is primarily affected by the inlet conditions of process and regeneration air, regeneration temperature and wheel speed. Therefore, subtropical climate conditions of Taxila city, Pakistan are considered to select the range of the temperature and absolute humidity in summer season as shown in fig. 3. It can be observed that temperature and absolute humidity beyond the comfort conditions varies from 15 °C to 40 °C and 12 g/kg-18 g/kg, respectively. Furthermore, comparison of each parameter with published data and validation with experimental data is presented.

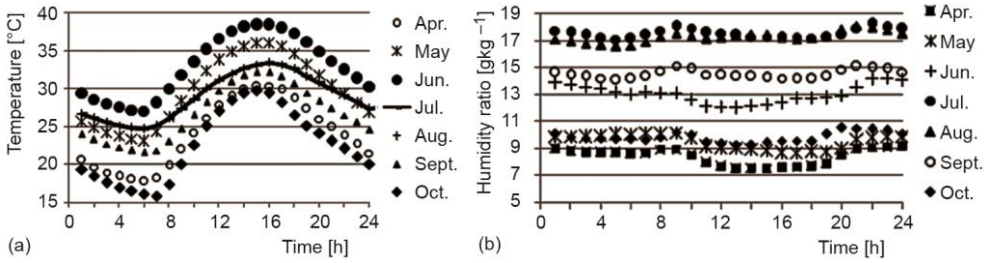

Figure 3. Subtropical climate of Taxila city, Pakistan in summer (a) temperature variation (b) absolute humidity variation

Parametric and experimental results with validation

Effect of inlet conditions of process air

The inlet parameters W_{sin} and T_{sin} of process air influence the properties of process air at outlet. The effect of W_{sin} on W_{sout} and ΔW is shown in fig. 4(a). The analysis is performed on different rotation speeds of the desiccant wheel *i. e.* 15, 26, and 36 rph. At higher values of W_{sin} moisture removal is higher. Thus, as the inlet humidity increases the amount of moisture removal is enhanced and represented as ΔW. Additionally, it can be seen that the dehumidification of air has higher value at lower rotation speed. This shows that the moisture removal capability of desiccant wheel decreases with increase of speed. Furthermore, the model results are compared with the previous published study of ASHRAE [25] as shown in fig. 4(b) and are in good agreement. Moreover, a comparison of experimental results along with model results are also shown in fig. 4(c). The proportional increase in W_{sin} results in the increase of W_{sout}. Furthermore, at lower values of W_{sin}, the moisture removal is less as compared to higher values of $W_{sin,}$ and maximum moisture removal is about 7.5 g/kg. The average

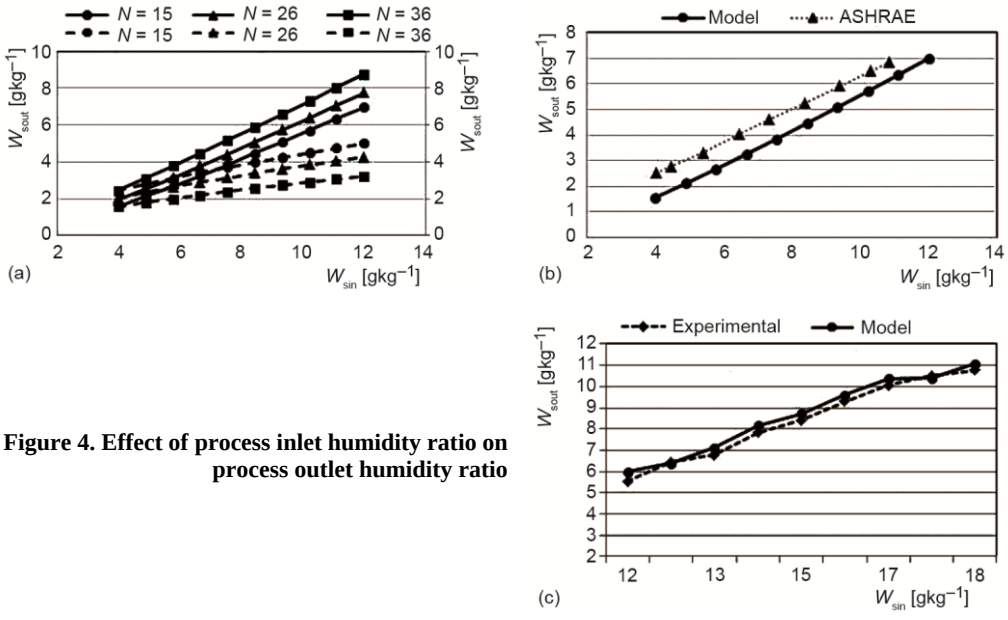

Figure 4. Effect of process inlet humidity ratio on process outlet humidity ratio

experimental value of W_{sout} is 8.48 g/kg and average W_{sout} from model results is 9.67 g/kg. Hence the difference in both average values is 1.27 g/kg.

Similarly, the effect of T_{sin} on the W_{sout} along with ΔW of the dehumidification process is shown in fig. 5(a). Moisture removal capacity is higher at lower values of T_{sin} and tends to decrease with higher values. The comparison of model results with the previous published study of ASHRAE [28] also exhibit similar trends as shown in fig. 5(b). Furthermore, validation of experimental data with model results is shown in fig. 5(c). The average model and experimental values of W_{sout} is 6.14 g/kg and 6.22 g/kg, respectively and are also in good agreement.

Additionally, W_{sin} also influences the T_{sout} as shown in fig. 6(a) along with ΔT. Here, T_{sout} of the process air rises with progressive enhancement in W_{sin} due to increased moisture removal in the process side. It can also be observed that ΔT of the air is higher at higher values of W_{sin} and lower values of N (rotation speed) of the wheel. Comparative results of the model with the previous published study of ASHRAE are presented in fig. 6(b).

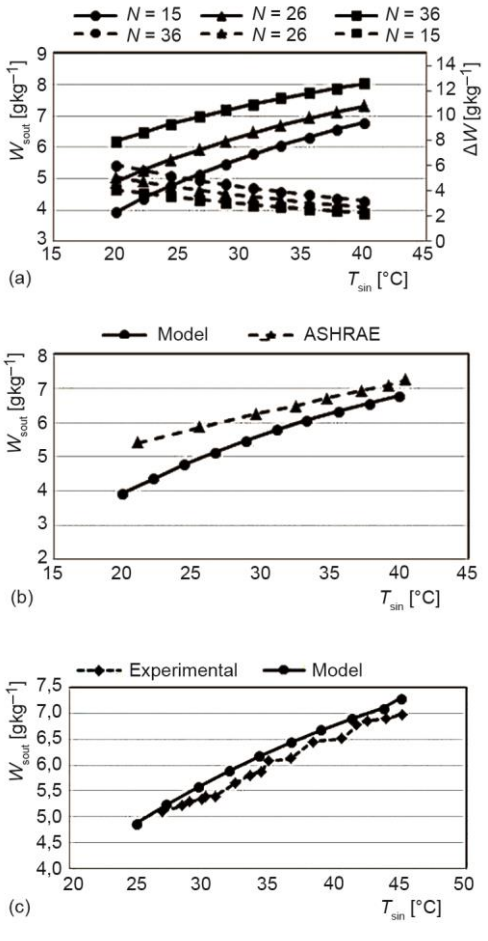

Figure 5. Effect of process inlet temperature on process outlet humidity ratio

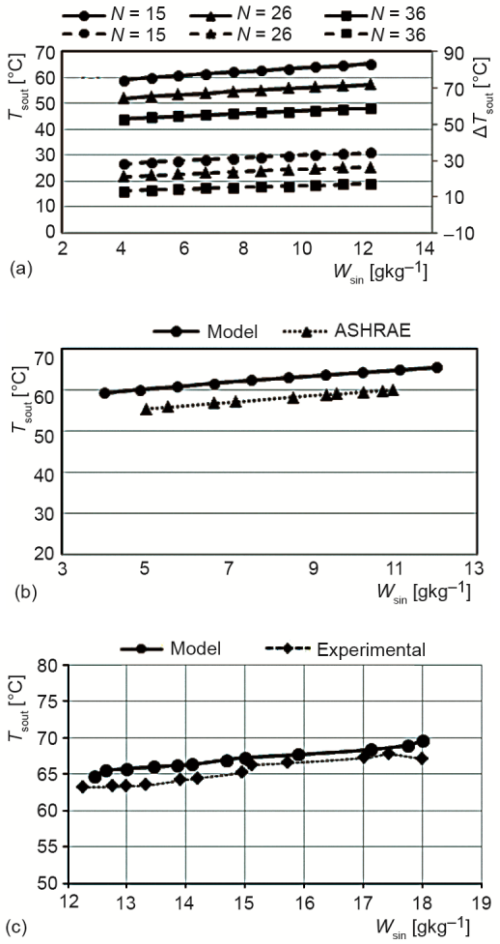

Figure 6. Effect of process inlet humidity ratio on process outlet temperature

Furthermore, experimental and model based outcomes to highlight the effect of W_{sin} on T_{sout} are shown in fig. 6(c). The average difference between experimental and model values of T_{sout} is 1.87 °C, and also in acceptable range.

Effect of inlet conditions of regeneration air

Regeneration air plays an important and critical role on the process air outlet conditions. The effect of T_{reg} on W_{sout} with ΔW is shown in fig. 7(a). Higher T_{reg}, higher the moisture removal capacity of desiccant material because desiccant wheel being better regenerated. On the other hand, the rotation speed also plays a key role on W_{sout}. The comparison of model results with the previous published study of ASHRAE for this parameter also exhibit similar trends as shown in fig. 7(b). However, the trend line concerning to ASHRAE data tends to straighten after regeneration temperature is further increased above 110 °C. Experimentally, the effect of T_{reg} on W_{sout} with validation is shown in fig. 7(c). The average W_{sout} obtained through experimentation is 6.83 g/kg while from model results is 6.13 g/kg. Hence, the difference in both average values is as low as 0.7 g/kg.

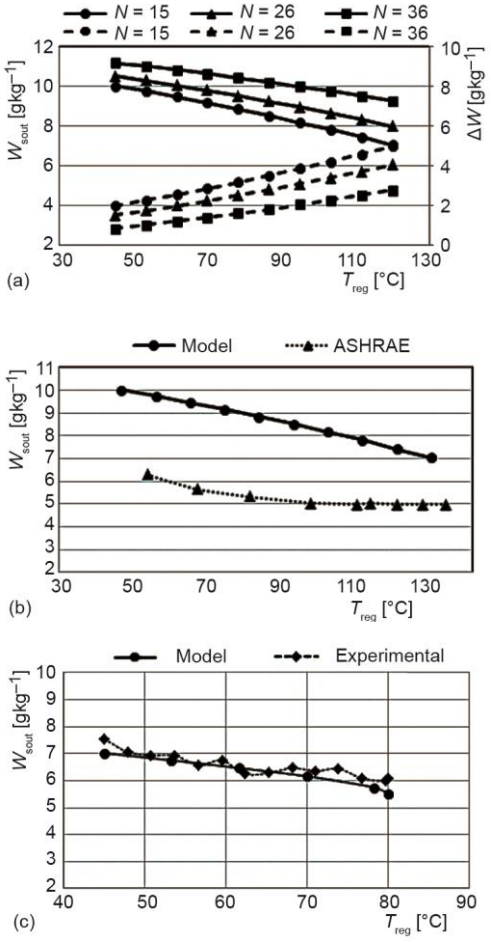

Figure 7. Effect of regeneration temperature on process outlet humidity ratio

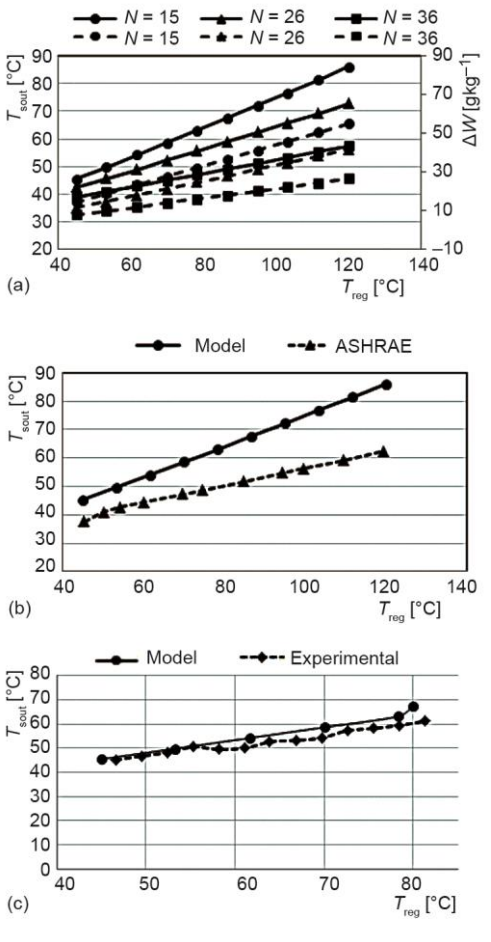

Figure 8. Effect of regeneration temperature on process outlet temperature

Additionally, the effect of T_{reg} on T_{sout} with ΔT is shown in fig. 8(a). It can be observed that, increases in T_{reg} increases T_{sout} due to the increased heat of adsorption with additional latent to sensible heat conversion.

At higher values of T_{reg} and lower values of N, difference of temperature ΔT of the process air dominates. The model results also exhibit similar trends when compared with ASHRAE as presented in fig. 8(b). While the experimentally determined effect of T_{reg} on T_{sout} along with model validation is shown in fig. 8(c) and the average experimental and model based values of T_{sout} are 54.24 °C and 58.7 °C, respectively.

Effect of wheel speed

This section deals with effect of wheel rotation speed, N, on the W_{sout} of the process outlet air with different W_{sin}, T_{sin}, and T_{reg}. The effect of speed, N, on W_{sout} along with ΔW at different W_{sin} is shown in fig. 9(a). The rotation speed plays a key role on dehumidification process. The ΔW increases with rotational speed till it reaches 17 rph, then decreases again. The reason is that at high speed wheel does not have sufficient time to remove moisture from the air. Additionally, ΔW of the air is low at low W_{sin} as compared to its higher values. Moreover, experimental results to study the effect of N on W_{sout} at different W_{sin} are also shown in fig. 9(b).

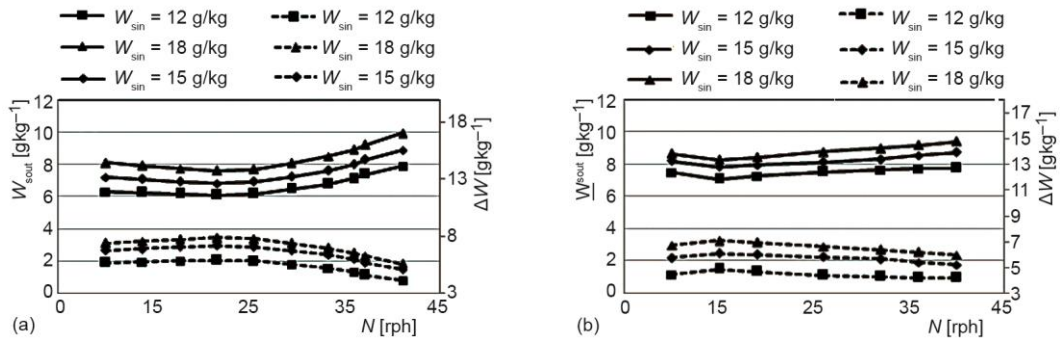

Figure 9. Effect of rotation speed of the wheel on process outlet humidity ratio with inlet humidity ratio; (a) model results, (b) experimental results

Moreover, the model based and experimental effects of the wheel speed on W_{sout} at different T_{sin} are also shown in figs. 10(a) and 10(b), respectively. At lower values of both T_{sin} and N, more moisture is removed by the wheel. The optimum speed for this parameter is around 15 rph and experimental results also validate the predicted value.

Furthermore, the effect of speed, N, on W_{sout} at different T_{reg} is shown in figs. 11(a) and 11(b). At high T_{reg} maximum moisture is removed by the wheel as compared to lower T_{reg} because it is easier to desorb the adsorbent. Similarly, higher values of N causes decrease in ΔW of the process air due to small time offered for regeneration. It can also be observed that optimum rotational speed is 15 rph.

Dehumidification effectiveness of desiccant wheel

Dehumidification effectiveness of desiccant wheel subjected to various inlet conditions of T_{sin}, W_{sin} and optimum wheel speed of 17 rph is presented in fig. 12. It can be observed that in fig. 12(a) effectiveness is low corresponding to lower values of W_{sin}. However,

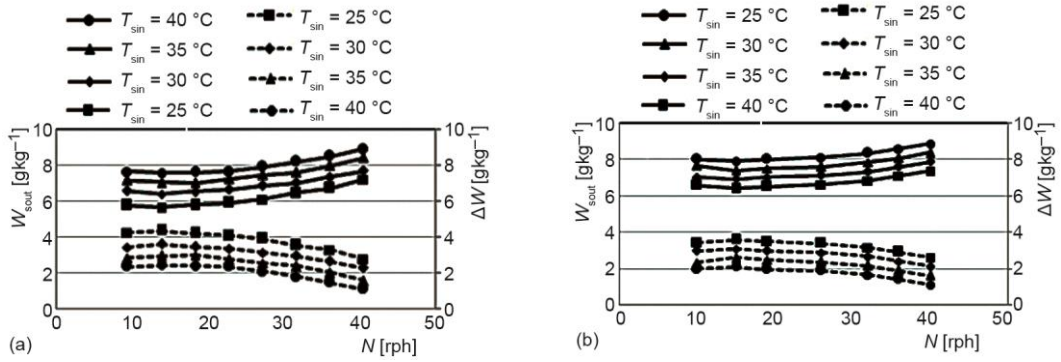

Figure 10. Effect of rotation speed of wheel on process outlet humidity ratio with process inlet temperature; (a) model results (b) experimental results

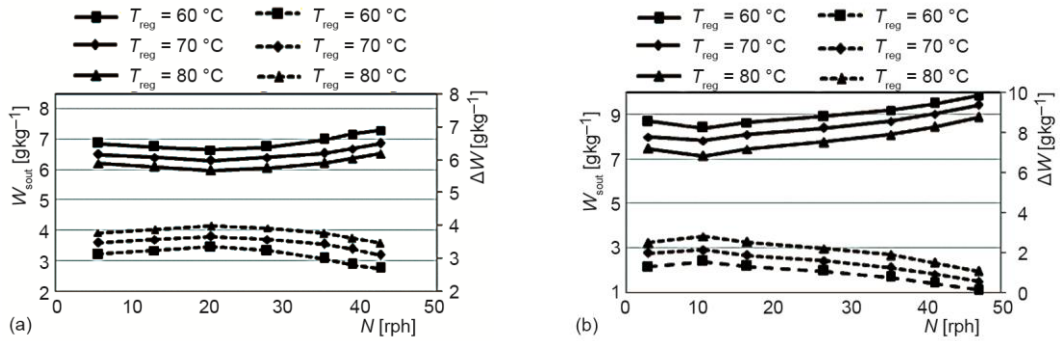

Figure 11. Effect of rotation speed of wheel on process outlet humidity ratio with regeneration temperature; (a) model results (b) experimental results

when W_{sin} increases effectiveness also increases till it reaches its peak. In this regard, the highest experimental value is 0.42. Similarly, experimental results to study the effect of regeneration temperature on effectiveness with different values of T_{sin} are presented in fig. 12(b). It shows that effectiveness of the desiccant wheel decreases when T_{sin} increases with positive impact of increasing regeneration temperatures. Moreover, comparison of experimental and model based results are shown in fig. 12(c). Both results are in good agreement with maximum root mean square error value of 3.2%.

Conclusions

The model based and experimental dehumidification performance analysis of solid desiccant wheel is evaluated for various design and climate parameters. Fundamental heat and mass transfer equations are used to predict the performance of the desiccant wheel for both process as well as regeneration sides. Furthermore, an experimental set-up is constructed at Renewable Energy Research and Development Center, Taxila city, Pakistan, for extensive experimental analysis and model validation. The experimental results showed a very good agreement with predicted model results for various critical parameters. Moreover, the developed model is capable to predict the drop in absolute humidity, temperature rise in process air, and actual desiccant wheel effectiveness with a good accuracy. Optimal rotational speed of

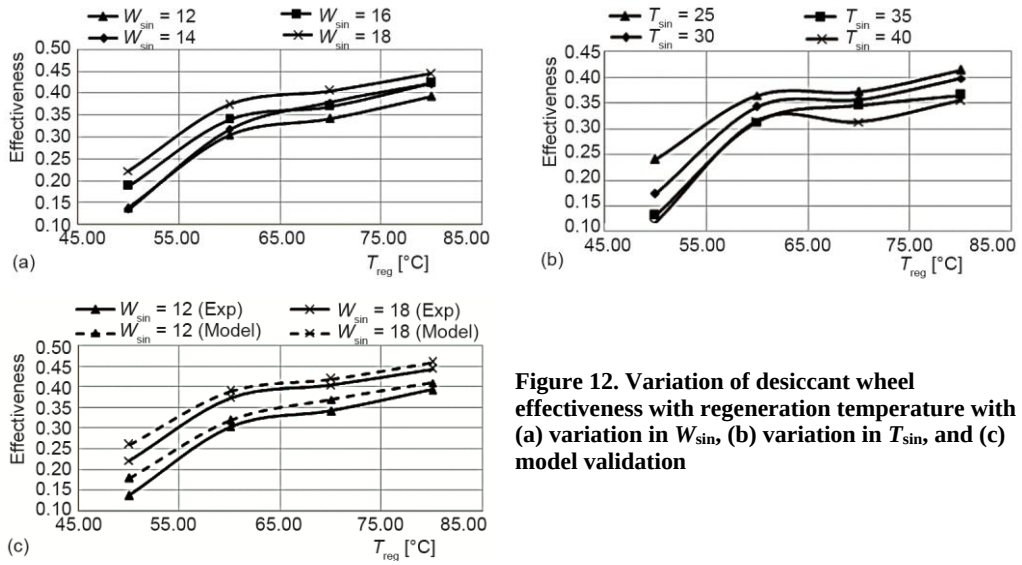

Figure 12. Variation of desiccant wheel effectiveness with regeneration temperature with (a) variation in W_{sin}, (b) variation in T_{sin}, and (c) model validation

the desiccant wheel ranges from 15-17 rph, due to strong dependence upon inlet conditions. Furthermore, dehumidification capacity and outlet temperature of the desiccant wheel increases with increase in inlet humidity. Maximum model based and experimental values for effectiveness are 0.45 and 0.43, respectively, at a regeneration temperature of 80 °C. While the resulted minimum and maximum root mean square error values for effectiveness are 2.1% and 3.2%, respectively.

Finally, the validated model can be further used for transient analysis of solar assisted desiccant evaporative cooling system.

Acknowledgment

Author wants to acknowledge the financial support of the research project by University of Engineering and Technology, Taxila city, Pakistan, under faculty research grant program.

Nomenclature

A_{ws} – surface area of desiccant wheel, [m^2/kg-wheel]
C – adsorption constant, [–]
C_{pc} – specific heat capacity, [$Jkg^{-1}K^{-1}$]
D – diameter of the wheel, [m]
D_{sf} – surface diffusivity, [m^2s^{-1}]
E_{at} – activation energy, [$kJkg^{-1}$]
H_1 – amount of sensible heat, [$kJkg^{-1}$]
h_{sin} – specific enthalpy of process air at inlet, [$kJkg^{-1}$]
h_{sout} – specific enthalpy of process air at outlet, [$kJkg^{-1}$]
I – radiation intensity, [Wm^{-2}]
L – wheel thickness, [mm]
$\dot{m}_s$ – mass-flow rate of process air, [kgh^{-1}]
N – rotation speed, [rph]
n – adsorption constant, [–]
Q_m – amount of water vapor absorbed by the wheel during an hour, [kgh^{-1}]
q – mass-flow rate of water vapor absorbed, [kgs^{-1}]
q_{eq} – amount of moisture absorbed, [kg]
R – gas constant, [$Jkg^{-1}K^{-1}$]
RH_{rin} – relative humidity of regeneration air at inlet, [%]
RH_{sin} – relative humidity of process inlet, [%]
S – cross sectional area of wheel, [m^2]
T_{reg} – regeneration temperature at inlet, [K]
T_{sin} – process inlet temperature, [K]
T_{sout} – process temperature at outlet, [K]
ΔT – temperature difference
t_1 – adsorption time, [s]
U_s – face velocity of air, [ms^{-1}]

W_{reg} – absolute humidity ratio of regeneration air at inlet, [kgkg^{-1}]
W_{sin} – absolute humidity ratio of process air at inlet, [kgkg^{-1}]
W_{sout} – absolute humidity ratio of process air at outlet, [kgkg^{-1}]
ΔW – difference in absolute humidity at inlet and outlet

Greek symbols

β_s – fractional area of each zone, [–]
ρ_a – density of air, [kgm^{-3}]
ρ_{ad} – density of adsorbent, [kgm^{-3}]
ρ_{dw} – density of desiccant wheel, [kgm^{-3}]
ε_d – dehumidification effectiveness, [–]

References

[1] Mijakowski, M., Sowa, J., An Attempt to Improve Indoor Environment by Installing Humidity-Sensitive air Inlets in a Naturally Ventilated Kindergarten Building, *Building and Environment, 111* (2017), Jan., pp. 180-191
[2] Kelly, M. O. *et al.*, Simulated Hygrothermal Performance of a Desiccant-Assisted Hybrid Air/Water Conditioning System in a Mixed Humid Climate under Dynamic Load, *Energy and Buildings, 86* (2015), Jan., pp. 45-57
[3] Straube, J. F., Moisture in Buildings, *ASHRAE Journal*, *44* (2002), 1 pp. 15-19
[4] Jani, D. B., *et al.*, Performance Studies of Hybrid Solid Desiccant-Vapor Compression Air-Conditioning System for Hot and Humid Climates, *Energy and Buildings, 102* (2015), Sep., pp. 284-292
[5] Bahman, A., *et al.*, Analysis of Energy Savings in a Supermarket Refrigeration/HVAC System, *Applied Energy, 98* (2012), Oct., pp. 11-21
[6] Xiao, F., Control Performance of a Dedicated Outdoor Air System Adopting Liquid Desiccant Dehumidification, *Applied Energy, 88* (2011), 1, pp. 143-149
[7] Wang, X., *et al.*, A Hybrid Dehumidifier Model for Real-Time Performance Monitoring, Control and Optimization in Liquid Desiccant Dehumidification System, *Applied Energy, 111* (2013), Nov., pp. 449-455
[8] Fauchoux, M., *et al.*, Testing and Modelling of a Novel Ceiling Panel for Maintaining Space Relative Humidity by Moisture Transfer, *International Journal of Heat and Mass Transfer, 53* (2010), 19-20, pp. 3961-3968
[9] Wang, N., Desiccant Wheel Thermal Performance Modeling for Indoor Humidity Optimal Control, *Applied Energy, 112* (2013), Dec., pp. 999-1005
[10] La, D., *et al.*, Technical Development of Rotary Desiccant Dehumidification and Air Conditioning: A Review, *Renewable and Sustainable Energy Reviews, 14* (2010), 1, pp. 130-147
[11] Shanmugam, V., Natarajan, E., Experimental Study of Regenerative Desiccant Integrated Solar Dryer with and without Reflective Mirror, *Applied Thermal Engineering, 27* (2007), 8-9, pp. 1543-1551
[12] Beccali, M., *et al.*, Simplified Models for the Performance Evaluation of Desiccant Wheel Dehumidification, *International Journal of Energy Research, 27* (2003), 1, pp. 17-29
[13] Beccali, M., *et al.*, Update on Desiccant Wheel Model, *International Journal of Energy Research, 28* (2004), 12, pp. 1043-1049
[14] Ruivo, C. R., Angrisani, G., The Effectiveness Method to Predict the Behaviour of a Desiccant Wheel: An Attempt of Experimental Validation, *Applied Thermal Engineering, 71* (2014), 2, pp. 643-651
[15] Kabeel, A. E., Solar Powered Air Conditioning System Using Rotary Honeycomb Desiccant Wheel, *Renewable Energy, 32* (2007), 11, pp. 1842-1857
[16] Niu, J. L., Zhang, L. Z., Effects of Wall Thickness on the Heat and Moisture Transfers in Desiccant Wheels for Air Dehumidification and Enthalpy Recovery, *International Communications in Heat and Mass Transfer, 29* (2002), 2, pp. 255-268
[17] Ali Mandegari, M., Pahlavanzadeh, H., Introduction of a New Definition for Effectiveness of Desiccant Wheels, *Energy, 34* (2009), 6, pp. 797-803
[18] Pandelidis, D., *et al.*, Comparison of Desiccant Air Conditioning Systems with Different Indirect Evaporative Air Coolers, *Energy Conversion and Management, 117* (2016), Jun., pp. 375-392
[19] Elgendy, E., Performance Enhancement of a Desiccant Evaporative Cooling System using Direct/Indirect Evaporative Cooler, *International Journal of Refrigeration, 51* (2015), Mar., pp. 77-87
[20] Uckan, I., Effect of Operation Conditions on the Second Law Analysis of a Desiccant Cooling System, *Applied Thermal Engineering, 113* (2017), Feb., pp. 1256-1265
[21] Sohani, A., *et al.*, A Novel Approach using Predictive Models for Performance Analysis of Desiccant Enhanced Evaporative Cooling Systems, *Applied Thermal Engineering, 107* (2016), Aug., pp. 227-252

[22] Cuce, P. M., Thermal Performance Assessment of a Novel Liquid Desiccant-Based Evaporative Cooling System: An Experimental Investigation, *Energy and Buildings, 138* (2017), Mar., pp. 88-95
[23] Gagliano, A., *et al.*, Performance Assessment of a Solar Assisted Desiccant Cooling System, *Thermal Science, 18* (2014), 2, pp. 563-576
[24] Ali, M., *et al.*, Development and Validation of a Desiccant Wheel Model Calibrated under Transient Operating Conditions, *Applied Thermal Engineering, 61* (2013), 2, pp. 469-480
[25] ***, ASHRAE,ASHRAE Handbook, *American Society of Heating, Refrigerating and Air-Conditioning Engineers*, Inc.: Atlanta, Geo, USA, 2009
[26] Kodama, A., *et al.*, Performance Evaluation for a Thermal Swing Honeycomb Rotor Adsorber using a Humidity Chart, *Journal of Chemical Engineering of Japan, 28* (1995), 1, pp. 19-24
[27] Kodama, A., *et al.*, The Use of Psychrometric Charts for the Optimisation of a Thermal Swing Desiccant Wheel, *Applied Thermal Engineering, 21* (2001), 16, pp. 1657-1674
[28] Kodama, A., *et al.*, Temperature Profile and Optimal Rotation Speed of a Honeycomb Rotor Adsorber Operated with Thermal Swing, *Journal of Chemical Engineering of Japan, 27* (1994), 5, pp. 644-649

Paper submitted: January 27, 2017
Paper revised: May 18, 2017
Paper accepted: July 7, 2017